HHS Public Access

Author manuscript

*J Mech Behav Biomed Mater*. Author manuscript; available in PMC 2018 November 01.

Published in final edited form as:

*J Mech Behav Biomed Mater*. 2017 November ; 75: 160–168. doi:10.1016/j.jmbbm.2017.07.017.

# COMPARISON OF FEMOROPOPLITEAL ARTERY STENTS UNDER AXIAL AND RADIAL COMPRESSION, AXIAL TENSION, BENDING, AND TORSION DEFORMATIONS

**Kaspars Maleckis**, **Paul Deegan**, **William Poulson**, **Cole Sievers**, **Anastasia Desyatova**, **Jason MacTaggart**[*], and **Alexey Kamenskiy**[*]

Department of Surgery, University of Nebraska Medical Center, Omaha, NE

## Abstract

High failure rates of Peripheral Arterial Disease (PAD) stenting appear to be associated with the inability of certain stent designs to accommodate severe biomechanical environment of the femoropopliteal artery (FPA) that bends, twists, and axially compresses during limb flexion. Twelve Nitinol stents (Absolute Pro, Supera, Lifestent, Innova, Zilver, Smart Control, Smart Flex, EverFlex, Viabahn, Tigris, Misago, and Complete SE) were quasi-statically tested under bench-top axial and radial compression, axial tension, bending, and torsional deformations. Stents were compared in terms of force-strain behavior, stiffness, and geometrical shape under each deformation mode. Tigris was the least stiff stent under axial compression (6.6, N/m axial stiffness) and bending (0.1 N/m) deformations, while Smart Control was the stiffest (575.3 N/m and 105.4 N/m, respectively). Under radial compression Complete SE was the stiffest (892.8 N/m), while Smart Control had the lowest radial stiffness (211.0 N/m). Viabahn and Supera had the lowest and highest torsional stiffness (2.2 μN·m/° and 959.2 μN·m/°), respectively. None of the 12 PAD stents demonstrated superior characteristics under all deformation modes and many experienced global buckling and diameter pinching. Though it is yet to be determined which of these deformation modes might have greater clinical impact, results of the current analysis may help guide development of new stents with improved mechanical characteristics.

### Keywords

femoropopliteal artery; peripheral arterial disease; stent; mechanical testing

## 1. INTRODUCTION

Peripheral Arterial Disease (PAD) affecting the femoropopliteal artery (FPA) is usually due to chronic atherosclerotic obstruction that reduces blood flow to the lower extremity. PAD affects more than 200 million individuals worldwide, and is associated with significant

[*]Corresponding authors. Department of Surgery 987690 Nebraska Medical Center Omaha, NE 68198-7690, Tel.: +1 (402) 559-5100; fax: +1 (402) 559-8985.

morbidity, mortality and decreased quality of life.(Fowkes et al., 2013) Endovascular stenting of the FPA is an increasingly popular minimally invasive procedure that utilizes Nickel-Titanium (NiTi) alloy-based self-expanding stents that form a metal scaffold in the artery to improve its patency after balloon angioplasty. Though FPA stenting is one of the most common procedures performed outside of the heart, it carries one of the highest rates of reconstruction failure, with many patients developing recurrent disease requiring re-intervention in as little as two years(Schillinger et al., 2007).

Although the mechanisms underlying endovascular reconstruction failure are likely multifactorial, it is believed that the dynamic mechanical environment of the FPA in the flexing limb contributes significantly to this process(Ansari et al., 2013; MacTaggart et al., 2014). Requirements for stent design are not well standardized, which may contribute to large variabilities in clinical outcomes as evidenced by industry-supported and industry-independent clinical trials demonstrating 43–83% one year patency rates(Rundback et al., 2015). Furthermore, studies demonstrate major differences in stent fracture rates(Higashiura et al., 2009; Scheinert et al., 2005; Werner, 2014), suggesting that stent design may play a major role in this process.

Empirically, ideal FPA stent designs need to accommodate tension/compression, bending, and torsion of the artery with minimal resistance, while also ensuring necessary resistance to radial compression and long-lasting fatigue performance. Though optimal stent evaluation should include clinical data, human research trials are challenging and require large sample sizes due to heterogeneity of PAD patient populations, differences in anatomical and lesion characteristics, and technical differences in procedures(Mohsen et al., 2013; Nakazawa et al., 2009; Scheinert et al., 2005). Benchtop mechanical stent testing allows direct evaluation of the device without the interference of patient-dependent factors, thereby eliminating the need for large sample sizes. While such tests do not necessarily replicate the complex loads and conditions experienced by the stent *in vivo*, they can be used to understand key mechanical characteristics of different designs, and these experimental data are critical for computer aided design work and validation of computational models.

Published benchtop mechanical studies are mostly limited to small numbers of stent models(Duda et al., 2000; Gong et al., 2004; Stoeckel et al., 2004; W. L. Gore & Associates, 2007), many of which are currently off the market or have been replaced with newer generation devices. In addition, FPA deformation magnitudes experienced with limb flexion, and therefore the loading conditions for the benchtop tests, have not been completely understood and quantified. Recent data on axial compression, bending and torsion of the FPA in walking, sitting and gardening postures (Desyatova et al., 2017; MacTaggart et al., 2014; Poulson et al., 2017), demonstrate that values of FPA deformations used for current stent design and preclinical testing(Ansari et al., 2013), may be significantly underestimated, potentially contributing to poor clinical performance of many FPA stents.

The goal of this study was to perform comprehensive benchtop mechanical comparison of 12 currently used PAD stents under the most severe deformations experienced by the FPA during flexion of the limb. Quantitative and qualitative head-to-head assessments of stent

performance under axial tension, axial compression, bending, radial compression, and torsion are detailed and the benefits and drawbacks of different stent designs are discussed.

## 2. METHODS

### 2.1. Stent models

Twelve stent models frequently used to treat PAD were mechanically tested under axial tension/compression, three-point bending, radial compression, and torsion deformations. Stents included Absolute Pro and Supera (both Abbott Vascular), Lifestent (Bard), Innova (Boston Scientific), Zilver (Cook), Smart Control and Smart Flex (both Cordis), EverFlex (Covidien), Viabahn and Tigris (both Gore), Misago (Terumo), and Complete SE (Medtronic). All stents were indicated for a 6mm artery, however the actual diameters ranged from 6.15 to 7.50 mm (average 6.99±0.45 mm). Since all stents pass quality checks after manufacturing, and fatigue behavior was not a part of the current study, one sample of each stent type was considered sufficient for quasi-static analysis. However, if the stent experienced plastic deformations under any of the testing modes, a new sample of the same dimensions was used for consecutive tests. This was the case with the Tigris stent that has polymer connectors that can undergo plastic deformations when overstretched.

### 2.2. General testing protocol

All stents were mechanically tested at 37°C. Stents were ~40mm in length and measurements were obtained in the middle of the sample, usually at least 5–10mm away from edges to minimize edge effects. Mechanical tests were performed in the same sequence for all stents: axial tension and compression, three-point bending, radial compression, and torsion. All tests were displacement-controlled and performed in a cyclic manner with ascending peak displacements. Only the last cycle with the highest peak deformation is presented in the results for each test. Peak displacements varied between stents due to some variation in span lengths and limitations of the load-cell capacity. Neutral positions of the Viabahn and Tigris stents were assumed with PTFE fabric and polymer interconnectors fully extended.

### 2.3. Axial tension and compression

Axial tension and compression tests were performed with CellScale biotester (Waterloo, Ontario, Canada) in displacement-controlled mode and in a temperature-controlled water bath. All stents were mounted on cylindrical supports and fixed around the perimeter with plastic barbed teeth clamps (Figure 1), which resulted in complete restriction of radial and torsional deformations at the supports. Span lengths between the supports varied from 19.5mm to 27.1mm. Tests were performed at 0.467mm/sec displacement rate and forces were measured with 2.5N, 5.0N, 10.0N, or 23N load cells, depending on the forces generated during the test. Axial stiffness was calculated for the linear and non-linear segments of the force-displacement curve as slopes of linear fit to the first and last 20% of the loading curve.

### 2.4. Three-point bending

Three-point bending tests were performed in a horizontal plane using the CellScale biotester. Stents were supported vertically by a 36.5mm wide smooth base plate, and horizontally by two 6mm-diameter pillars located 34mm apart, with no restriction on rotation or lateral displacement (Figure 1). Deformation was applied to the mid-span of the stent through a 10mm high and 6.35mm wide rounded-tip loading pin. Displacement-controlled tests were performed in a temperature controlled water bath with 1.0mm/sec displacement rates. Forces were measured with 2.5N or 5.0N load cells. Bending stiffness was calculated similarly to the axial stiffness, but using the first and the last 30% of the force-displacement curve.

### 2.5. Radial compression

Radial compression tests were performed with 40mm wide v-shaped clamps mounted on the force transducers of the CellScale biotester (Figure 1). No external supports were used for the stents. Cyclic tests with 1mm, 2mm, 3mm, 4mm, and 5mm travel of v-clamps were performed with 0.125mm/sec displacement rates on stent sections placed in a heated water bath and displacements of the v-clamps were used to calculate reduction of the cross-section assuming that stent remained circular. Forces were measured with 5N, 10N, or 23N load cells. Radial stiffness was calculated similarly to the axial stiffness using the first and last 20% of the curve.

### 2.6. Torsion

Torsion tests were performed in a temperature-controlled air chamber using a TA Electroforce 5175 BioDynamic tester (New Castle, DE, USA) equipped with a 2.82 Nm torsional load cell. Stents were mounted using tapered supports and were fixed with a non-adhesive Parafilm tape. The tape completely restricted stent deformations at the supports. The average span between the supports was 23.0±1.4 mm which corresponds to the distance between intra-arterial markers used to measure limb flexion-induced FPA torsion(Desyatova et al., 2017) (Figure 1). During the test axial deformations were restricted. Consecutive cyclic tests with 30°/cm, 45°/cm, 60°/cm, 75°/cm, and 90°/cm maximum rotations in both clockwise and counterclockwise directions were performed at 5°/sec rotational speed. Torsional stiffness was calculated similarly to the bending stiffness using the first and the last 30% of the torque-rotation curve.

## 3. RESULTS

### 3.1. Axial tension and compression

Axial tension test results are summarized in Figure 2. Panel A provides force (N) – strain (%) relations under tension up to 160% of initial length, while panel B compares stiffness (N/m) of all stents in tension. Viabahn, Smart Flex, Tigris, and Smart Control stent responses in tension were non-linear, while other stents demonstrated mostly linear behavior (Figure 2A). At 11% strain Tigris stent started developing significant plastic deformation within its polymer interconnectors, and the associated yielding load was ~5N. Viabahn and Smart Flex stents became stiffer with increasing loads, while the Smart Control stent became softer. The highest stiffness in tension was demonstrated by the Viabahn (12,387 N/m) and

the Smart Flex (2,469 N/m) stents. The lowest stiffness in tension was shown by the Misago (32 N/m), Absolute Pro (47 N/m), and Supera (94 N/m) stents.

Stiffness in compression was overall smaller than stiffness in tension (Figure 3). While for most stents the difference was within 5%, SmartFlex, Tigris and Viabahn stents were 1.5, 23, and 102-fold less stiff in compression than in tension. The SmartControl stent was the stiffest in compression (575 N/m), followed by the SmartFlex (534 N/m), Zilver (236 N/m) and EverFlex (218 N/m) stents. The least stiff stents were Tigris and Viabahn (7 N/m), followed by the Misago (31 N/m) and the Supera (45 N/m) stents.

Innova, Zilver, Smart Control, Smart Flex, and EverFlex stents buckled before reaching 25% compressive strain which represents the intersubject mean compression magnitude experienced by the popliteal artery (PA) in the gardening posture(Poulson et al., 2017) (Figure 3C, negative sign indicates compression). The Complete SE stent buckled exactly at 25% and LifeStent buckled at 39%, which corresponds to intersubject maximum PA compression(Poulson et al., 2017). The Viabahn and Misago stents could withstand compressive strains of 41% and 43% without buckling. The Tigris stent did not show any signs of buckling when compressed to 33%, but it was not compressed further to avoid plastic deformation in its interconnectors. The Absolute Pro and Supera stents did not buckle even when compressed beyond 50% strain.

Structural geometric changes under axial tension and compression are visualized in Figure 4 for each stent. The Smart Flex stent demonstrated a significant focal reduction in lumen diameter under tension and an increase in diameter under compression.

### 3.2. Three-point bending

Similar to axial tension and compression, three-point bending results were significantly different among stent designs (Figure 5). In general, stents were significantly less stiff under bending loads compared to tension or compression. The highest bending stiffness was observed in the Smart Control (98 N/m) stent, followed by the SmartFlex (54 N/m), and EverFlex (46 N/m) stents. The least stiff stents under bending loads were the Tigris (2 N/m), Viabahn (3 N/m) and Misago (10 N/m) devices. Load-pin displacements higher than 5mm resulted in sliding of some stents at supports as can be seen from Figure 5A by the change in slope of the force-displacement curves. Stent geometries at 10 mm load-pin displacement are presented in Figure 6, which corresponds to approximately 119° bending angle. Intersubject mean and maximum values of the bends experienced by the PA in the gardening posture were reported as 136° and 117° (Poulson et al., 2017) which corresponds to ~6.9mm and ~10.4mm load pin displacements respectively (Figure 5A). The Innova, Zilver, Smart Control, EverFlex and Complete SE stents kinked or pinched at the middle of the span due to the interaction with the load-pin. The Absolute Pro and (to a lesser extent) Misago and Zilver stents demonstrated a “gator-back” appearance at bending.

### 3.3. Radial compression

Response to radial compression is presented in Figure 7. Maximum radial pinching of the PA is marked with a vertical line at 87.6% of the stent cross-sectional area(Ansari et al., 2013). Most stents were stiffer under radial compression than under axial compression or

bending. All stents were able to be compressed such that less than 40% of their initial cross-sectional area remained open, except the Supera stent that was compressed to only 81% of the initial area before the force reached the limit on the 23N loadcell. The Supera device demonstrated appreciable non-linearity in its radial compression response. It demonstrated modest radial stiffness (295 N/m) when compressed preserving 90% of the initial cross-sectional area, but the stiffness increased exponentially (to 11,261 N/m) when more radial compression was applied. The opposite behavior was observed for the LifeStent, Innova, SmartControl, EverFlex, Misago, and Complete SE stents. These stents lost most of their radial stiffness when they were compressed beyond 65–70% of their initial cross-sectional area. A moderate drop in stiffness under large radial compression was also observed for the Absolute Pro and Viabahn stents, while stiffness of the Zilver, Smart Flex, and Tigris stents increased with more radial compression.

### 3.4. Torsion

Responses of stents to clockwise rotation are presented in Figure 8A. Declines in slopes of the torque (Nmm) – rotation (°/cm) curves correspond to the occurrence of global buckling. The LifeStent, Smart Flex, Viabahn, Tirgis and Misago stents had non-symmetric designs and demonstrated different responses when twisted clockwise (+) and counterclockwise (-). Responses of non-symmetric stents to rotation are demonstrated in Figure 8B, and images of these stents rotated to ±45°/cm are presented in Figure 8E. Though the Viabahn and Tigris stents also had non-symmetric (spiral) designs, their responses under clockwise and counterclockwise rotations were similar and no differences in their shapes were observed. Viabahn and Tigris stents also developed plastic deformations at rotations above 20–40°/cm, which reduced the resistance to torsion on subsequent cycles. Figure 8B illustrates development of these plastic deformations at large rotations.

The torsional stiffness of all stents under both clockwise and counterclockwise rotations is plotted in Figure 8C. The Supera (959 μN·m/°), SmartControl (87 μN·m/°), and Smart Flex (58 μN·m/°) stents demonstrated the highest torsional stiffness, while the Viabahn (2 μN·m/°), Absolute Pro (9 μN·m/°) and Tigris (13 μN·m/°) stents demonstrated the lowest.

The majority of stents buckled before reaching the maximum prescribed twist of 90°/cm, and some demonstrated significant decreases in diameter. Stents that could withstand 90°/cm rotation without buckling were the Absolute Pro, Innova, Zilver, Viabahn, and Tigris stents (Figure 8D). The Smart Control, Misago and Complete SE stents could withstand 43°/cm rotation without buckling – a value reported to represent maximum rotation of the PA in the gardening posture(Desyatova et al., 2017). For the LifeStent and SmartFlex stents, the ability to withstand the largest PA twist depended on twist direction. The Supera and EverFlex stents buckled at 3°/cm and 43°/cm, but for the Supera stent, this was associated with significant torque as demonstrated in Figure 8A. All stents except the Supera could withstand the intersubject mean PA rotation of 26°/cm experienced in the gardening posture(Desyatova et al., 2017). Stents experiencing 45°/cm and 90°/cm twists are demonstrated in Figure 9.

## 4. DISCUSSION

High failure rates of FPA interventions are often attributed to severe mechanical deformations that occur with limb movement (Ansari et al., 2013). These deformations include axial tension/compression, bending, radial compression, and torsion. Current stents may be pushed beyond their limits when exposed to these hostile mechanical conditions within the flexing limb. Inability of a device to withstand limb flexion-induced deformations may result in device failure or disruption of the healing response with repetitive injury to the arterial wall. While it is challenging to study this process *in vivo*, it is possible to compare performance of different FPA stents in a bench-top setting by simulating the major modes of FPA deformation. To our knowledge, the current study is the first comprehensive head-to-head bench-top assessment of FPA stent behavior under limb flexion-induced deformations. It was performed with 12 commercially available and currently used devices, providing a perspective on the mechanical characteristics of each design.

Since stents are deployed when the limb is in its straight configuration and the FPA is pre-stretched(Kamenskiy et al., 2016a), it is unlikely that stents experience much axial tension when the limb is flexed(MacTaggart et al., 2014; Poulson et al., 2017). Axial compression however can be quite severe, reaching as high as 39% in the acutely flexed limb that results from the gardening posture(Poulson et al., 2017). The lower resistance of stents to axial compression may be beneficial as it provides flexibility and may create a less adverse interaction with the arterial wall. We note that FPA stent behavior is different from balloon-expandable stainless steel or cobalt chromium coronary stents that are not designed to deform with the artery. On the contrary, the purpose of FPA superelastic nitinol stents is to accommodate arterial deformations while ensuring minimal arterial injury and preservation of vessel patency. The Viabahn, Tigris, Misago, and Supera stents demonstrated the least resistance to axial compression, while the Smart Control, Smart Flex, and Zilver stents had the most resistance. The behavior of the Smart Flex stent under axial compression demonstrated twist-stretch coupling due to its unique asymmetric design. It is possible that significant focal diameter changes observed during axial deformations were influenced by restriction at the supports, and *in vivo* conditions might make these changes more subtle and uniform over the length of the stent.

Most of the stents experienced buckling before reaching 39% compressive strain, with only four devices (Absolute Pro, Supera, Viabahn, and Misago) able to withstand it. It is not clear whether the Tigris stent is able to withstand this level of compression without buckling since it was not compressed beyond 33% to avoid plastic deformation of the polymer connectors. Though it is yet to be seen whether buckling is reduced or exacerbated *in vivo*, the observed behavior provides a general understanding that high axial stiffness may be associated with this effect. Stent buckling *in vivo* may affect lumen diameter, damage the arterial wall, and contribute to quicker stent failure. Results of axial compression testing described here agree with data previously published by Gore(W. L. Gore & Associates, 2007) using 6mm diameter stents and an internal support rod to limit buckling. At 15% compression Gore reported 1.99N, 0.54N, 0.53N, and 0.17N resistances for Smart Control, Absolute Pro, LifeStent, and Viabahn stents, respectively. These values are on average 0.19 N higher than those reported here, possibly due to the influence of the support rod.

The ability of stents to accommodate severe bending deformations during limb flexion may also minimize interaction between the arterial wall and the device, possibly reducing arterial wall injury and local stress concentrations in the stent. Three-point bending tests demonstrated that in general stents could bend easier than they could axially compress, but there was an expected strong positive correlation (Pearson correlation $r = 0.91$, $p<0.01$) between stiffness in bending and stiffness in axial compression. The Viabahn and Tigris stents demonstrated the smallest resistances to both bending and axial compression, while Smart Control stent was the stiffest of all devices demonstrating the highest resistance to both axial compression and bending. Direct comparison of these results to those previously published (W. L. Gore & Associates, 2007) is challenging due to differences in span lengths and endpoint measures. However, the overall trend was similar with the highest resistances observed for the Smart Control stent, followed by the LifeStent, Absolute Pro, and Viabahn devices.

The Absolute Pro, Misago, and Zilver stents exhibited “gator-back” appearances on the outer surface during bending, which is likely a result of their long and acutely angled struts. While presence of the artery around the stent would likely mask this effect, strut protrusion may cause focal injury as sharp stent edges dig into the arterial wall. The Innova, Zilver, Smart Control, EverFlex, and Complete SE stents exhibited a different effect during bending: they demonstrated local diameter pinching. While it is not clear whether this behavior was caused purely by the load-pin or is an intrinsic bending characteristic of these stents, this scenario may potentially be negative in highly tortuous arteries when severe pinching may obstruct blood flow.

While low axial and bending stiffness are likely beneficial to ensure stent flexibility, radial stiffness determines the ability of the stent to prevent arterial collapse after angioplasty. Higher, rather than lower, radial stiffness is usually considered a desirable characteristic, particularly in highly calcified lesions that produce significant radial resistance. The Supera stent was significantly different than all of the other stents in this category, but its stiffness increased dramatically only after the stent’s original cross-sectional area was reduced by more than 10%. This effect was consistent across different Supera stent diameters and lengths (results are not included in this manuscript), and could be caused by the initial sliding of the stent wires that are held together by friction. It is important to note that the radial stiffness of the Supera stent strongly depends on axial extension. While the ends of the stent were free to elongate under the radial compression test performed here, this may or may not be the case *in vivo*. The Supera stent loses its radial stiffness when significantly elongated, an effect that appears to be important as demonstrated in the clinical literature(Garcia et al., 2015).

Apart from the Supera stent, the Complete SE, LifeStent, and Viabahn stents demonstrated high radial stiffness, while the Smart Control and Zilver stents were relatively weak radially. These results are different from the parallel plate pinch tests previously published (W. L. Gore & Associates, 2007) that reported approximately 1.50 N, 1.13 N, 1.47 N, and 1.23 N reaction forces for the Smart Control, Absolute Pro, Lifestent, and Viabahn devices when compressed to 25% of their initial diameter. Our data demonstrates 1.08 N, 1.34 N, 1.2 N, and 2.54 N reaction forces at similar compressions, indicating higher resistance of the

Viabahn stent and lower resistance of the Smart Control stent to radial compression. These discrepancies may stem from differences in testing equipment and protocol. Note, that compression around the entire circumference of the stent is likely more desirable than compression at 4 discrete points produced by the V-clamps because it provides more uniform force distribution; however, since all stents were tested using the same methodology, stent ranking in terms of radial compression was likely captured correctly. While more radial stiffness is generally desired in a properly sized stent, it is not clear how much radial force is needed *in vivo*. Significantly oversized stents with high radial stiffness can produce appreciable chronic outward force that may cause unnecessary injury to the arterial wall.

Torsion was the last mode of FPA deformations considered in this study. The FPA twists significantly with limb flexion, particularly in its popliteal location(Desyatova et al., 2017; MacTaggart et al., 2014). Though most stents are indicated for the proximal segment of the FPA, the superficial femoral artery, they are often used in the popliteal artery because this area is commonly affected by atherosclerotic disease(Watt, 1965). The superficial femoral artery was shown to twist as much as 13–20°/cm in the gardening posture, while 26–43°/cm twists were reported in the PA(Desyatova et al., 2017). Torsional assessment of stents demonstrated that most devices were capable of accommodating significant PA rotations; however some buckled even under relatively mild twists. Inability of FPA stents to accommodate limb flexion-induced rotations without buckling could contribute to arterial wall or device damage, while significant torsional stiffness can restrict rotation in the stented segment and potentially exacerbate it at the stent ends. The highest resistance to torsion was demonstrated by the Supera, Smart Control and Smart Flex stents, while the lowest torsional resistance was observed in the Viabahn, Absolute Pro, and Tigris devices. Direct comparison of these results to those previously published (W. L. Gore & Associates, 2007) is challenging due to differences in test setups and endpoint measures; however the overall trend is similar with the Smart Control stent demonstrating higher torsional stiffness than the Viabahn, LifeStent and Absolute Pro stents.

Several stent designs (LifeStent, SmartFlex, Misago) demonstrated different torsional characteristics when rotated clockwise and counterclockwise. Since distribution of torsion is non-uniform along the length of the FPA, and direction of twist can alternate substantially(Desyatova et al., 2017), the benefits or drawbacks of non-symmetric stent designs are yet to be understood. Furthermore, certain non-symmetric designs possess significant coupling of rotation and radial deformations, where the stent diameter expands or contracts depending on the direction of twist. It has yet to be studied how these diameter alterations affect chronic outward radial force and flow patterns in the artery *in vivo*.

Although some stents performed better than others in one or multiple deformation modes, none of the stents showed superiority under all deformations. Figure 10 summarizes the results for torsion, bending, axial and radial compression testing in one graph. Stiffness in compression, bending and torsion is plotted on the X, Y and Z axes, while size of the markers (normalized by a factor of 25 for convenience) indicates radial stiffness. Though Figure 10 provides a visual comparison of devices, it is yet to be determined which of the

deformation modes are more important clinically, and whether location and lesion-specific selection of stents could be beneficial for improving their clinical performance.

Results of this study should be viewed in the context of its limitations. First and foremost, bench-top tests do not fully recapitulate the *in vivo* environment of the FPA. Stents *in vivo* are slightly compressed radially due to oversizing and they deform in tandem with the arterial wall and the surrounding tissues. It is common practice to perform bench-top tests in silicone tubes to simulate the *in vivo* environment, but this approach is also not perfect. Most importantly, properties of silicone are significantly different from those of the artery wall and these tubes cannot account for the wide inter-patient variation in arterial mechanics(Kamenskiy et al., 2016b). Computational analysis is perhaps a better alternative that can take into account the interpatient variability and also provide stress distributions associated with a particular deformation. Validation of computational models with bench-top experiments is perhaps best performed when the experiments are straightforward, such as those described here.

The second limitation is assumption that FPA deformations are driven by displacements rather than force. The nature of these deformations remain to be more fully understood, as both tethering arterial branches and surrounding tissues likely have significant effects. In the meantime it should be remembered that load-controlled (as opposed to displacement-controlled) tests can produce different results. This for example could be the case for the Supera stent that buckled under displacement-controlled rotation, but this buckling was associated with significant torque.

The third limitation is concerned with the testing techniques and variation in sample diameters. For example, stents in radial compression were loaded through the v-clamps that applied load at discrete locations rather than along the entire circumference of the stent. This resulted in collapse of the stent at higher compression levels, similar to the pinch test with parallel plates. While some pinching produced by asymmetric atherosclerotic plaques is likely taking place *in vivo*, the load that arterial wall imposes on the stent surface is likely more uniformly distributed throughout the circumference. Other examples are the boundary conditions at the stent ends. During torsion and axial deformation tests, stents were restricted to axial movement, while during radial compression and bending the ends were free. Under *in vivo* conditions stents likely experience combined and complex loading modes, which may affect the conclusions obtained with simple bench-top tests.

It is also important to remember that low resistance to axial compression, bending, and torsion and high radial strength are not the only mechanical characteristics that determine stent performance. For example, fatigue characteristics are of critical importance, but they were not analyzed in this study. The incidence of material fatigue and stent fracture appears to be much more frequent in FPA stents; however it is likely not the only factor contributing to reconstruction failure since most patients with FPA restenosis do not have fractures in their stents (Kurayev et al., 2014; Werner, 2014). Nevertheless, Higashiura et al(Higashiura et al., 2009) reported more stent fractures in the FPA than in less dynamic iliac arteries, and Iida et al(Iida et al., 2006) showed strong correlation between stent fracture and exercise frequency. Fatigue analysis requires lengthy experiments and large numbers of samples, and

therefore will be a focus of future studies. This current work however can help improve the design of fatigue testing techniques and protocols and enhance data analysis in the context of quasi-static performance.

A variety of other factors, not directly related to the Nitinol stent, can also influence device performance. For example, the ePTFE fabric attached to the Nitinol skeleton is not permeable and can alter the collateral flow that occurs through small arterial side branches. Increased outflow through the entire stent, or portions of the stent, may have an important effect on influencing stent patency. Device delivery systems can be another factor that affects stent performance. The Supera stent in particular seems to be very sensitive to axial elongation determined by the delivery technique, which may significantly reduce radial strength and clinical efficacy of the device.

Lastly, true stent performance should ultimately be assessed through human clinical trials. However, since loading conditions experienced by stents *in vivo* include a combination of deformation modes, bench-top experiments can provide insights into what occurs *in vivo*. The results presented here are not intended to replace these trials and as we do not yet know the relative importance of each of the deformation modes in determining stent-artery interaction and the resultant biological and clinical responses, we cannot suggest that one stent or another is superior or inferior. Instead, these results demonstrate the need for more head-to-head comparisons of peripheral devices with bench-top testing, computational modeling, and *in vivo* performance data to arrive at an optimal design for this particular peripheral arterial location. In the meantime, this comprehensive head-to-head bench-top analysis of commercially available FPA stents provides an understanding on which devices may be better suited to accommodate compression, bending, and torsion observed in human FPA during limb flexion.

## 5. CONCLUSIONS

FPA stents are significantly different in their mechanical responses to modes of arterial deformation that occur with limb flexion. High radial stiffness and low resistance to axial compression, bending and torsion are likely beneficial for FPA stent performance, as this allows the stent to maintain lumen diameter in diseased arteries, while allowing the stented segment to follow deformations that occur naturally with limb flexion. Although some stents performed better than others in one or multiple deformation modes, none of the stents showed superiority under all deformations. It is yet to be determined which of the deformation modes have higher clinical importance, and whether certain stent designs perform better in particular FPA segments.

## Acknowledgments

This research was supported in part by the NHLBI R01 HL125736, F32 HL124905, and Mary and Dick Holland Regenerative Medicine Program.

## References


Ansari F, Pack LK, Brooks SS, Morrison TM. Design considerations for studies of the biomechanical environment of the femoropopliteal arteries. J. Vasc. Surg. 2013; 58:804–813. DOI: 10.1016/j.jvs.2013.03.052 [PubMed: 23870198]

Desyatova A, Poulson W, Deegan P, Lomneth C, Seas A, Maleckis K, MacTaggart J, Kamenskiy A. Limb flexion-induced twist and associated intramural stresses In the human femoropopliteal artery. J. R. Soc. Interface. 2017; 14 doi:http://dx.doi.org/10.1098/rsif.2017.0025.

Duda SH, Wiskirchen J, Tepe G, Bitzer M, Kaulich TW, Stoeckel D, Claussen CD. Physical properties of endovascular stents: an experimental comparison. J. Vasc. Interv. Radiol. 2000; 11:645–54. [PubMed: 10834499]

Fowkes FGR, Rudan D, Rudan I, Aboyans V, Denenberg JO, McDermott MM, Norman PE, Sampson UK, Williams LJ, Mensah GA, Criqui MH, Lozano R, Naghavi M, Foreman K, Vos T, Flaxman A, Naghavi M, Nations, U., Affairs, D. of E. and S., Anonymous; Stoffers H, Rinkens P, Kester A, Kaiser V, Knottnerus J, Hirsch A, Criqui M, Treat-Jacobson D, McDermott M, Fried L, Simonsick E, Ling S, Guralnik J, Pande R, Perlstein T, Beckman J, Creager M, Smith G, Shipley M, Rose G, Fowkes F, Murray G, Butcher I, Collaboration, the A.B.I.; Yusuf S, Reddy S, Ounpuu S, Anand S, Medicine, I. of, Nations, U., Organization, W.H.; Aboyans V, Criqui M, Abraham P, Disease, A.H.A.C. on P.V., Prevention, C. on E. and, Cardiology, C. on C., Nursing, C. on C., Intervention, C. on C.R. and, Anesthesia, C. on C.S; Hiatt W, Hoag S, Hamman R, Murabito J, Evans J, Nieto K, Larson M, Levy D, Wilson P, Selvin E, Erlinger T, Ostchega Y, Paulose-Ram R, Dillon C, Gu Q, Hughes J, Rooks R, Simonsick E, Miles T, Criqui M, Vargas V, Denenberg J, Makdisse M, Pereira A, Brasil D, Cardiology/Funcor, the H. of B.S. and P.A.D.C. of the B.S.; Makdisse M, Ramos L, Moreira F, Buitrón-Granados L, Martínez-López C, Peña JE la, Guerchet M, Aboyans V, Mbelesso P, Fowkes F, Thorogood M, Connor M, Lewando-Hundt G, Tzoulaki I, Tollman S, Sigvant B, Wiberg-Hedman K, Bergqvist D, Eldrup N, Sillesen H, Prescott E, Nordestgaard B, Kröger K, Stang A, Kondratieva J, Group, the H.N.R.S; Carbayo J, Divisón, J., Escribano, J., (GEVA), the G. de E.V. de A; Ramos R, Quesada M, Solanas P, Investigators, the R; Fowler B, Jamrozik K, Norman P, Allen Y, Fujiwara T, Saitoh S, Takagi S, Hozawa A, Ohmori K, Kuriyama S, Garofolo L, Barros N, Miranda F, D'Almeida V, Cardien L, Ferreira S, Chuang S-Y, Chen C-H, Cheng C-M, Chou P, He Y, Jiang Y, Wang J, Fan L, Li X, Hu F, Woo J, Lynn H, Wong S, Kweon S-S, Shin M-H, Park K-S, Sritara P, Sritara C, Woodward M, Premalatha G, Shanthirani S, Deepa R, Markovitz J, Mohan V, Subramaniam T, Nang E, Lim S, Lee Y-H, Shin M-H, Kweon S-S, Kim J, Jeon Y, Cho S, Sinning C, Wild S, Schulz A, Alzamora M, Forés R, Baena-Díez J, group, the P. study; Wang Y, Li J, Xu Y, An W, Xian L, Zhao L, Detrano R, Criqui M, Wu Y, Ohnishi H, Sawayama Y, Furusyo N, Maeda S, Tokunaga S, Hayashi J, Blanes J, Cairols M, Marrugat J, ESTIME, the, Bank, T.W.; Bank TW, Vock D, Atchison E, Legler J, Rudan I, Tomaskovic L, Boschi-Pinto C, Campbell H, Group, W.H.E.R., Organization, W.H; Rothman K, Greenland S, Aboyans V, Criqui M, McClelland R, Stoffers H, Kester A, Kaiser V, Rinkens P, Kitslaar P, Knottnerus J, Olin J, Dachun X, Jue L, Liling Z, O'Hare A, Katz R, Shlipak M, Cushman M, Newman A, Dumville J, Lee A, Smith F, Fowkes F, McDermott M, Liu K, Greenland P, McDermott M, Greenland P, Liu K, McDermott M, Guralnik J, Tian L, Kannel W, Skinner J, Schwartz M, Shurtleff D, Danaei G, Finucane M, Lin J, Pressure), the G.B. of M.R.F. of C.D.C.G. (Blood; Danaei G, Finucane M, Lu Y, Glucose), the G.B. of M.R.F. of C.D.C.G. (Blood; Farzadfar F, Finucane M, Danaei G, (Cholesterol), the G.B. of M.R.F. of C.D.C.G.; Giovino G, Mirza S, Samet J, Group, the G.C. et al. Comparison of global estimates of prevalence and risk factors for peripheral artery disease in 2000 and 2010: a systematic review and analysis. Lancet. 2013; 382:1329–1340. DOI: 10.1016/S0140-6736(13)61249-0 [PubMed: 23915883]

Garcia L, Jaff MR, Metzger C, Sedillo G, Pershad A, Zidar F, Patlola R, Wilkins RG, Espinoza A, Iskander A, Khammar GS, Khatib Y, Beasley R, Makam S, Kovach R, Kamat S, Leon LRJ, Eaves WB, Popma JJ, Mauri L, Donohoe D, Base CC, Rosenfield K. Wire-Interwoven Nitinol Stent Outcome in the Superficial Femoral and Proximal Popliteal Arteries: Twelve-Month Results of the SUPERB Trial. Circ. Cardiovasc. Interv. 2015; 8:1–8. DOI: 10.1161/CIRCINTERVENTIONS.113.000937

Gong X, Pelton A, Duerig T. Finite element analysis and experimental evaluation of superelastic Nitinol stent. and Superelastic. 2004

Higashiura W, Kubota Y, Sakaguchi S, Kurumatani N, Nakamae M, Nishimine K, Kichikawa K. Prevalence, factors, and clinical impact of self-expanding stent fractures following iliac artery stenting. J. Vasc. Surg. 2009; 49:645–652. DOI: 10.1016/j.jvs.2008.10.019 [PubMed: 19268770]

Iida O, Nanto S, Uematsu M, Morozumi T, ichi Kotani J, Awata M, Onishi T, Ito N, Sera F, Minamiguchi H, Akahori H, Nagata S. Effect of exercise on frequency of stent fracture in the superficial femoral artery. Am J Cardiol. 2006; 98:272–274. [PubMed: 16828607]

Kamenskiy A, Seas A, Bowen G, Deegan P, Desyatova A, Bohlim N, Poulson W, MacTaggart J. In situ longitudinal pre-stretch in the human femoropopliteal artery. Acta Biomater. 2016a; 32:231–237. DOI: 10.1016/j.actbio.2016.01.002 [PubMed: 26766633]

Kamenskiy A, Seas A, Deegan P, Poulson W, Anttila E, Sim S, Desyatova A, MacTaggart J. Constitutive description of human femoropopliteal artery aging. Biomech. Model. Mechanobiol. 2016b; In press. doi: 10.1007/s10237-016-0845-7

Kurayev A, Zavlunova S, Babaev A. CRT-207 Role of Nitinol Stent Fractures in the Development of In-Stent Restenosis in the Superficial Femoral Artery. JACC Cardiovasc. Interv. 2014; 7:S35.doi: 10.1016/j.jcin.2014.01.089

MacTaggart J, Phillips N, Lomneth C, Pipinos I, Bowen R, Baxter B, Johanning J, Longo G, Desyatova A, Moulton M, Dzenis Y, Kamenskiy A. Three-Dimensional Bending, Torsion and Axial Compression of the Femoropopliteal Artery During Limb Flexion. J Biomech. 2014; 47:2249–2256. [PubMed: 24856888]

Mohsen MK, Alqahtani A, suwaidi J Al. Stent fracture: How frequently is it recognized? Hear. Views. 2013; 14:72–81.

Nakazawa G, Finn AV, Vorpahl M, Ladich E, Kutys R, Balazs I, Kolodgie FD, Virmani R. Incidence and Predictors of Drug-Eluting Stent Fracture in Human Coronary Artery. A Pathologic Analysis. J. Am. Coll. Cardiol. 2009; 54:1924–1931. DOI: 10.1016/j.jacc.2009.05.075 [PubMed: 19909872]

Poulson W, Kamenskiy A, Seas A, Deegan P, Lomneth C, MacTaggart J. Limb Flexion-Induced Axial Compression and Bending in Human Femoropopliteal Artery Segments. J. Vasc. Surg. 2017 Accepted.

Rundback JH, Herman KC, Patel A. Superficial Femoral Artery Intervention: Creating an Algorithmic Approach for the Use of Old and Novel (Endovascular) Technologies. Curr. Treat. Options Cardiovasc. Med. 2015; 17:400.doi: 10.1007/s11936-015-0400-3 [PubMed: 26265117]

Scheinert D, Scheinert S, Sax J, Piorkowski C, Bräunlich S, Ulrich M, Biamino G, Schmidt A. Prevalence and clinical impact of stent fractures after femoropopliteal stenting. J Am Coll Cardiol. 2005; 45:312–315. [PubMed: 15653033]

Schillinger M, Sabeti S, Dick P, Amighi J, Mlekusch W, Schlager O, Loewe C, Cejna M, Lammer J, Minar E. Sustained benefit at 2 years of primary femoropopliteal stenting compared with balloon angioplasty with optional stenting. Circulation. 2007; 115:2745–9. DOI: 10.1161/CIRCULATIONAHA.107.688341 [PubMed: 17502568]

Stoeckel D, Pelton A, Duerig T. Self-expanding nitinol stents: material and design considerations. Eur. Radiol. 2004; 14:292–301. DOI: 10.1007/s00330-003-2022-5 [PubMed: 12955452]

Gore WL. Associates, I. Mechanical Properties of Nitinol Stents and Stent-grafts: Comparison of 6mm Diameter Devices. 2007

Watt J. Origin of femoro-popliteal occlusions. Br. Med. J. 1965; 2:1455–1459. [PubMed: 5849435]

Werner M. Factors Affecting Reduction in SFA Stent Fracture Rates. Endovasc. Today. 2014:93–95.

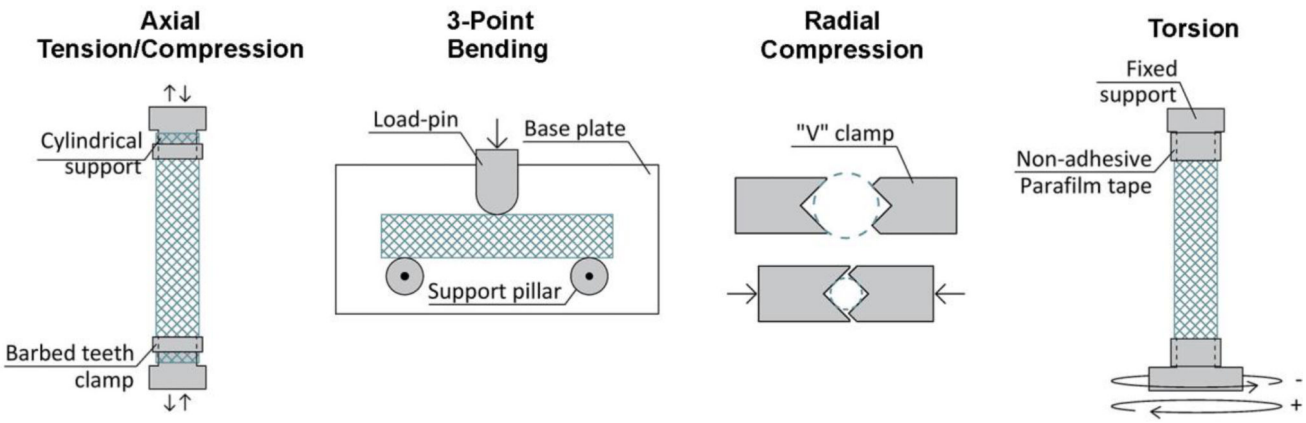


**Fig 1.**

Schematic of the bending, axial tension/compression, torsion and radial compression tests performed in this study.

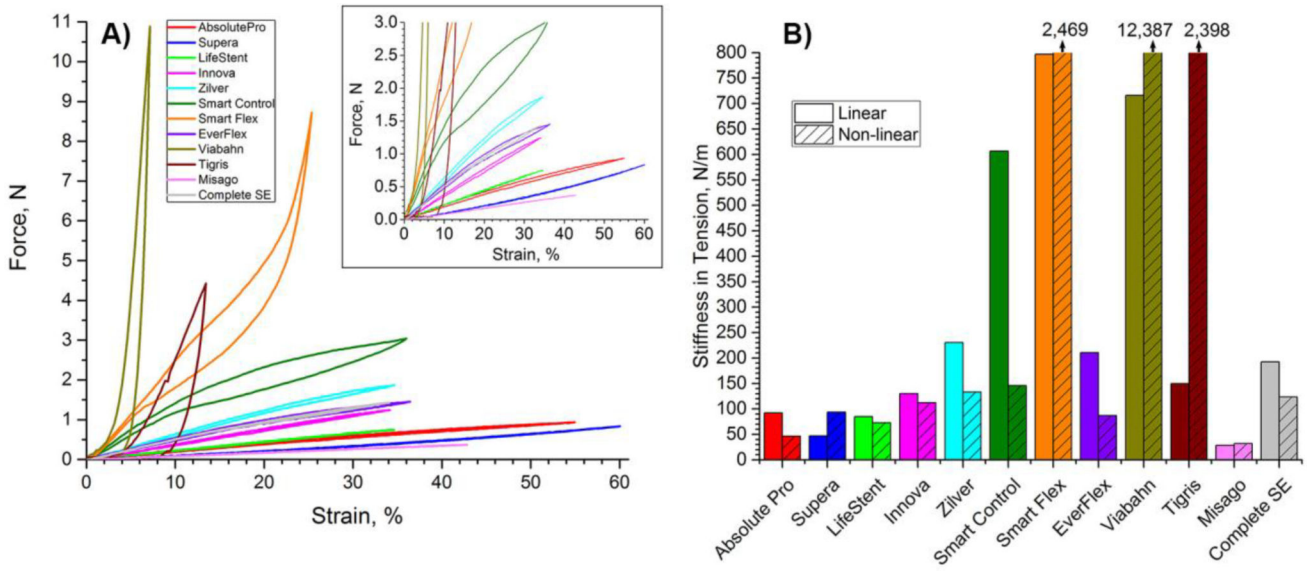


**Fig 2.**

Behavior of stents under axial tension. A) force (N) – strain (%) relations; B) stiffness in tension (N/m) calculated for the linear and non-linear regions of the force-strain response. Stiffness of SmartFlex and Viabahn stents are listed on top of their respective columns. The Tigris stent developed plastic deformations after ~11% strain.

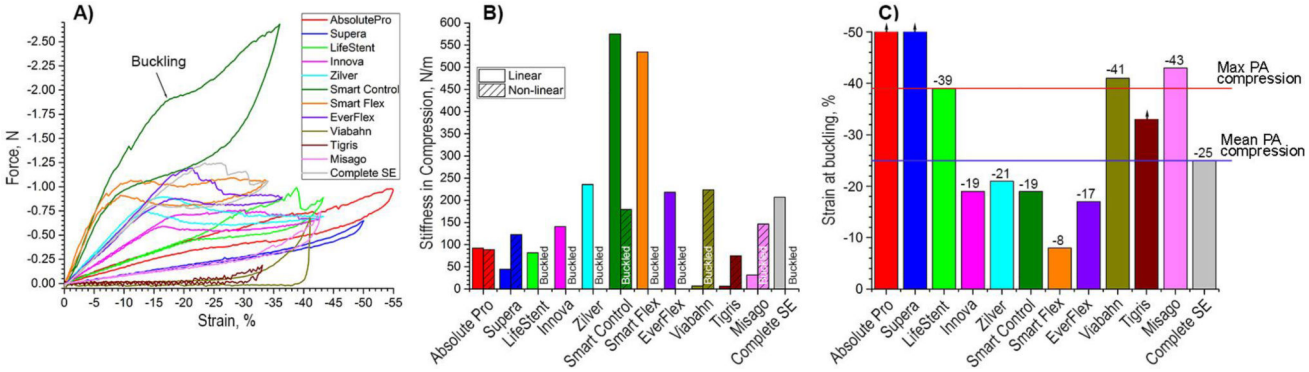


**Fig 3.**

Behavior of stents under axial compression. A) Force (N) – strain (%) response; B) Stiffness in compression (N/m) calculated for the linear and non-linear segments of force-strain response. The non-linear segment of the graph for most stents corresponds to buckled configuration; C) Occurrence of global buckling under axial compression. Intersubject mean and maximum values of the largest axial compression experienced by the popliteal artery (PA) in the gardening posture are marked with horizontal lines drawn at −25% and −39% strains(Poulson et al., 2017). Negative sign indicates compressive strain. Absolute Pro and Supera stents did not buckle at compression beyond 50%, and Tirgis did not buckle at 33% compression.

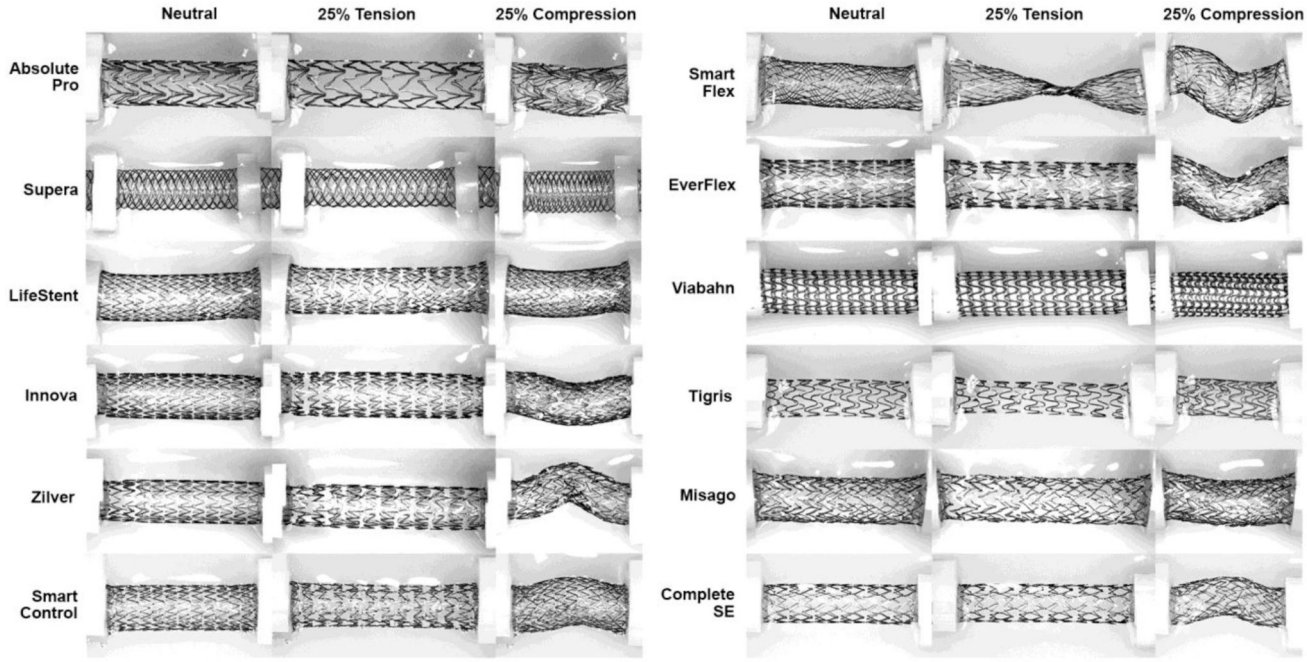


**Fig 4.**

Stents in the neutral position, under 25% axial tension, and 25% axial compression.

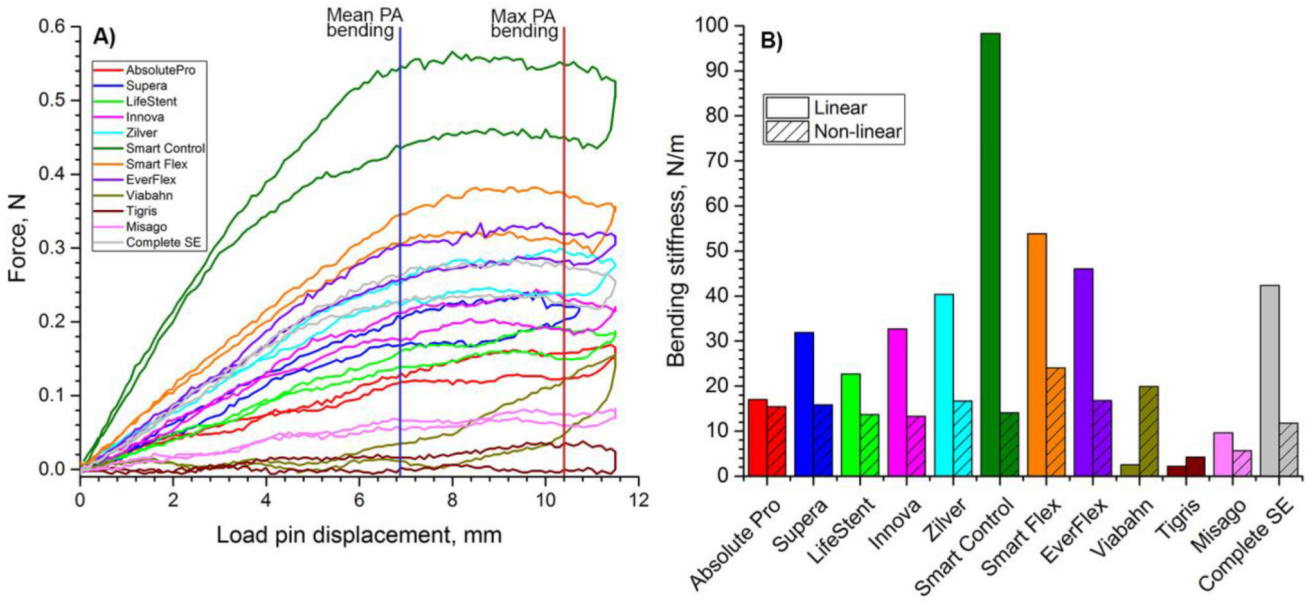


**Fig 5.**

A) Three-point bending behavior of stents. Intersubject mean and maximum values of the most severe bends experienced by the popliteal artery (PA) in the gardening posture are marked with vertical blue and red lines drawn at 6.9mm and 10.4mm load pin displacements(Poulson et al., 2017); B) Bending stiffness (N/m) for the linear and non-linear segments of force - load pin displacement responses.

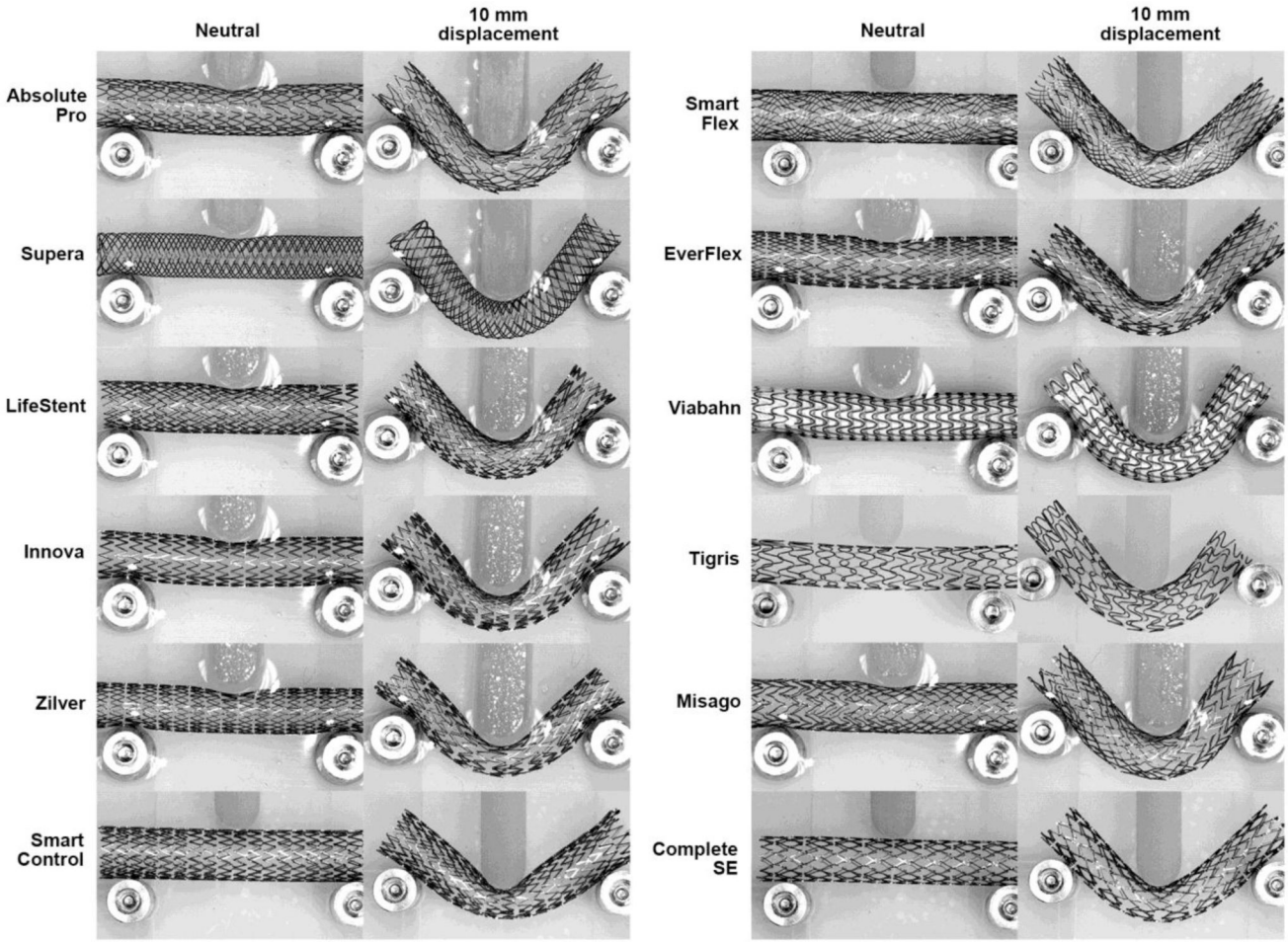


**Fig 6.**

Stents under three-point bending in the neutral position and loaded with 10mm load pin displacement applied to the middle of the span. Note “gator-back” appearance of the Absolute Pro, Misago, and Zilver stents, and pinched diameters of the Innova, Zilver, Smart Control, EverFlex, and Complete SE stents.

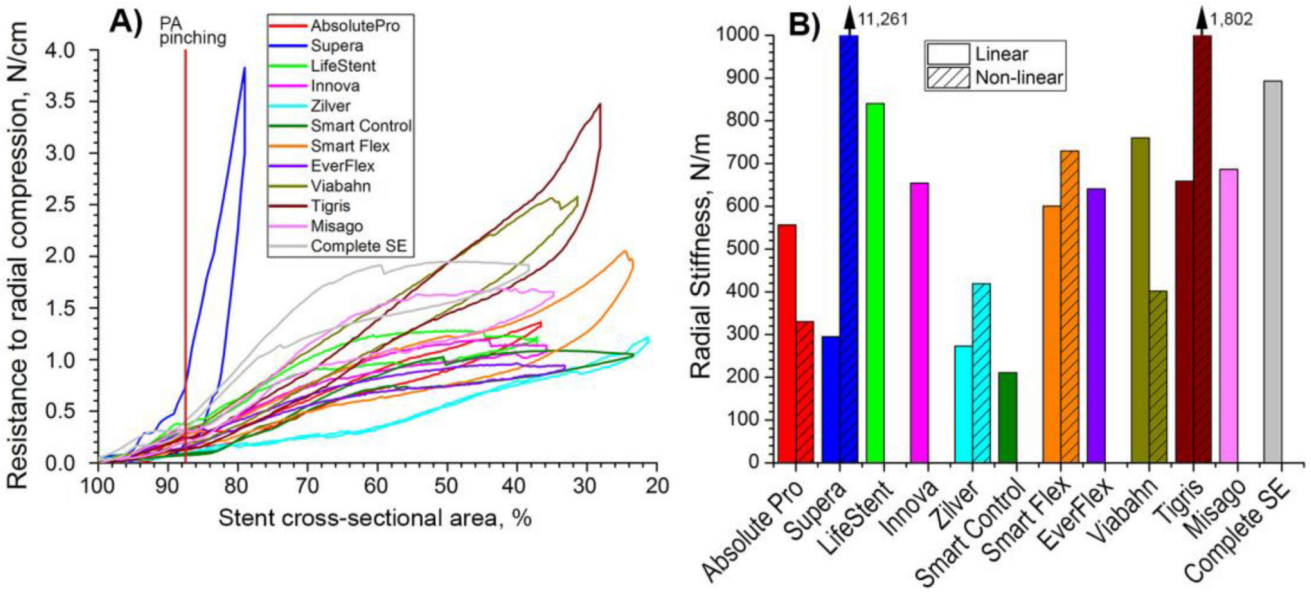


**Fig 7.**

A) Radial compression (N/cm) as a function of stent cross-sectional area (%). Supera stent was compressed only to 81% of its initial cross-sectional area because the load exceeded the limit on the 23N load cell. Maximum PA pinching is marked with a vertical red line at ~88% of stent cross-sectional area(Ansari et al., 2013); B) Radial stiffness (N/m) normalized to 1cm length of the stent and calculated for linear and non-linear segments of graphs in panel A. Note that some stents lost most of their radial stiffness when compressed more than 65–70% of their initial cross-sectional area, resulting in zero column heights in panel B.

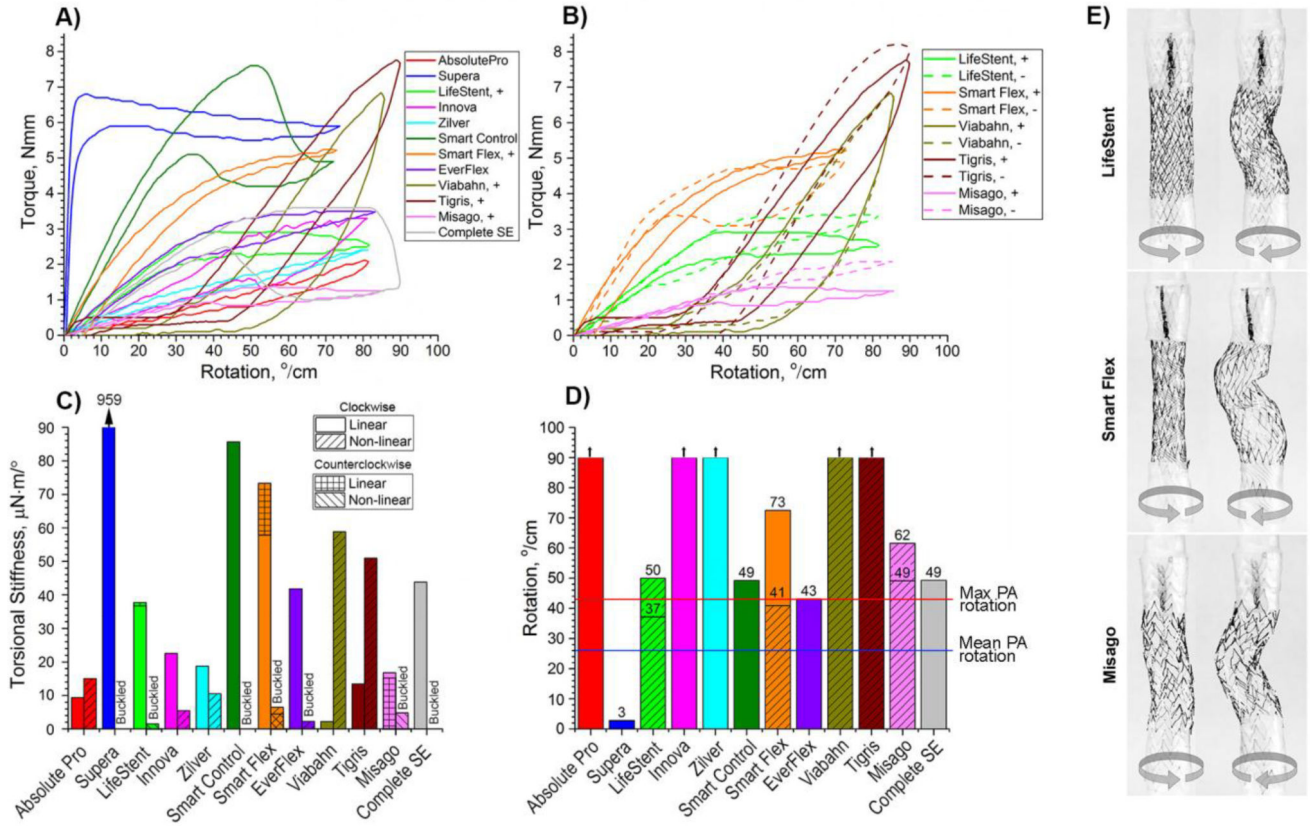


**Fig 8.**

Behavior of stents under torsional loads. A) Torque (Nmm) – rotation (°/cm) relations for clockwise (+) twist; B) Torque (Nmm) – rotation (°/cm) relations for both clockwise (+) and counterclockwise (-) rotations for non-symmetric stents; C) Torsional stiffness (µN·m/°) calculated for linear and non-linear regions in panel A. Non-symmetric LifeStent, SmartFlex and Misago devices had different values in clockwise and counterclockwise twists which are marked accordingly; D) Maximum rotation that stents can withstand before buckling. Absolute Pro, Innova, Zilver, Viabahn and Tigris stents did not buckle within 0 to 90°/cm rotation range. Intersubject mean and maximum values of the largest rotation experienced by the Popliteal Artery (PA) in the gardening posture(Desyatova et al., 2017) are marked with blue and red horizontal lines at 26°/cm and 43°/cm respectively; E) Non-symmetric LifeStent, SmartFlex and Misago stents experienced buckling differently when rotated clockwise and counterclockwise. Images are presented for ±45°/cm rotations.

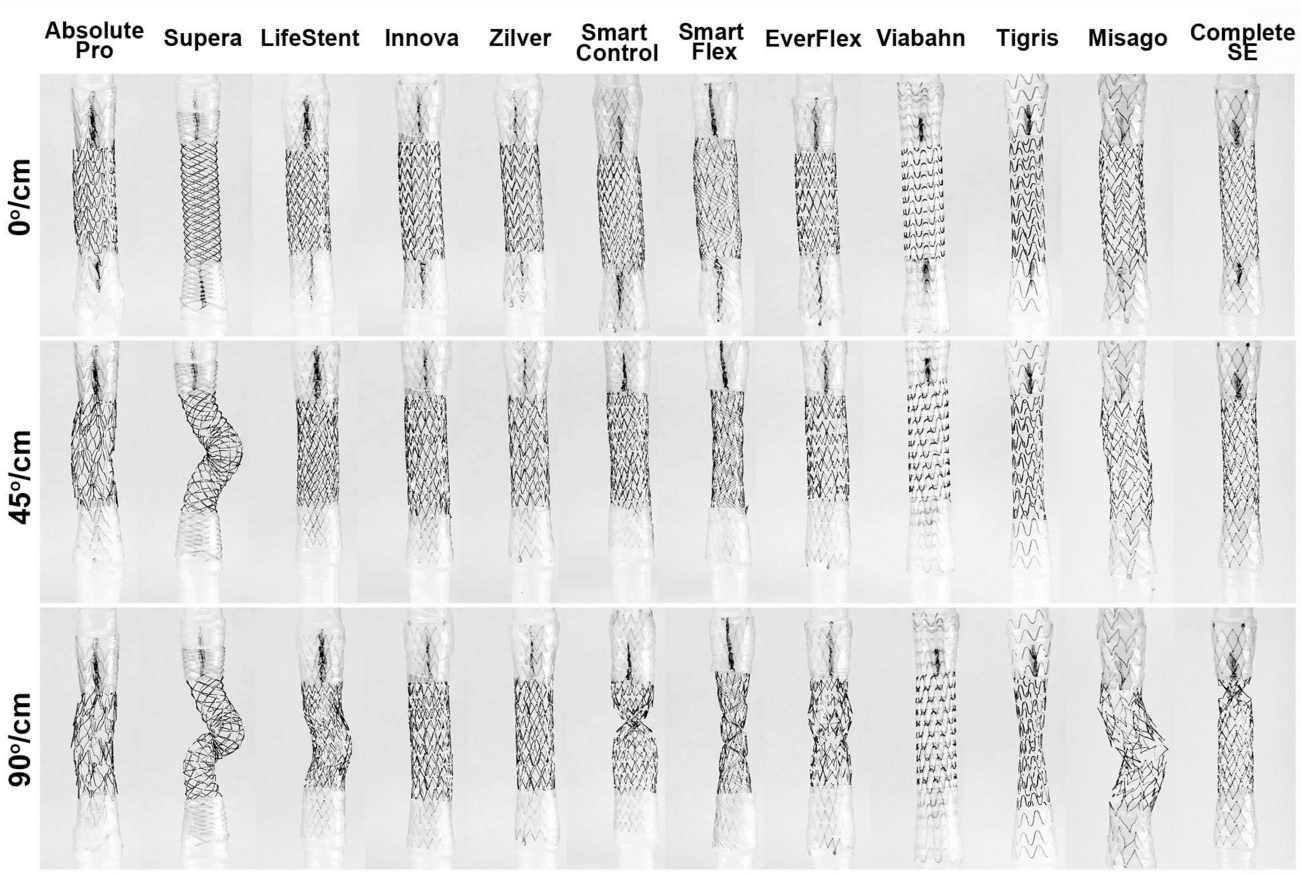


**Fig 9.**

Stents in their unloaded configuration (0°/cm) and under 45°/cm and 90°/cm counterclockwise rotations.

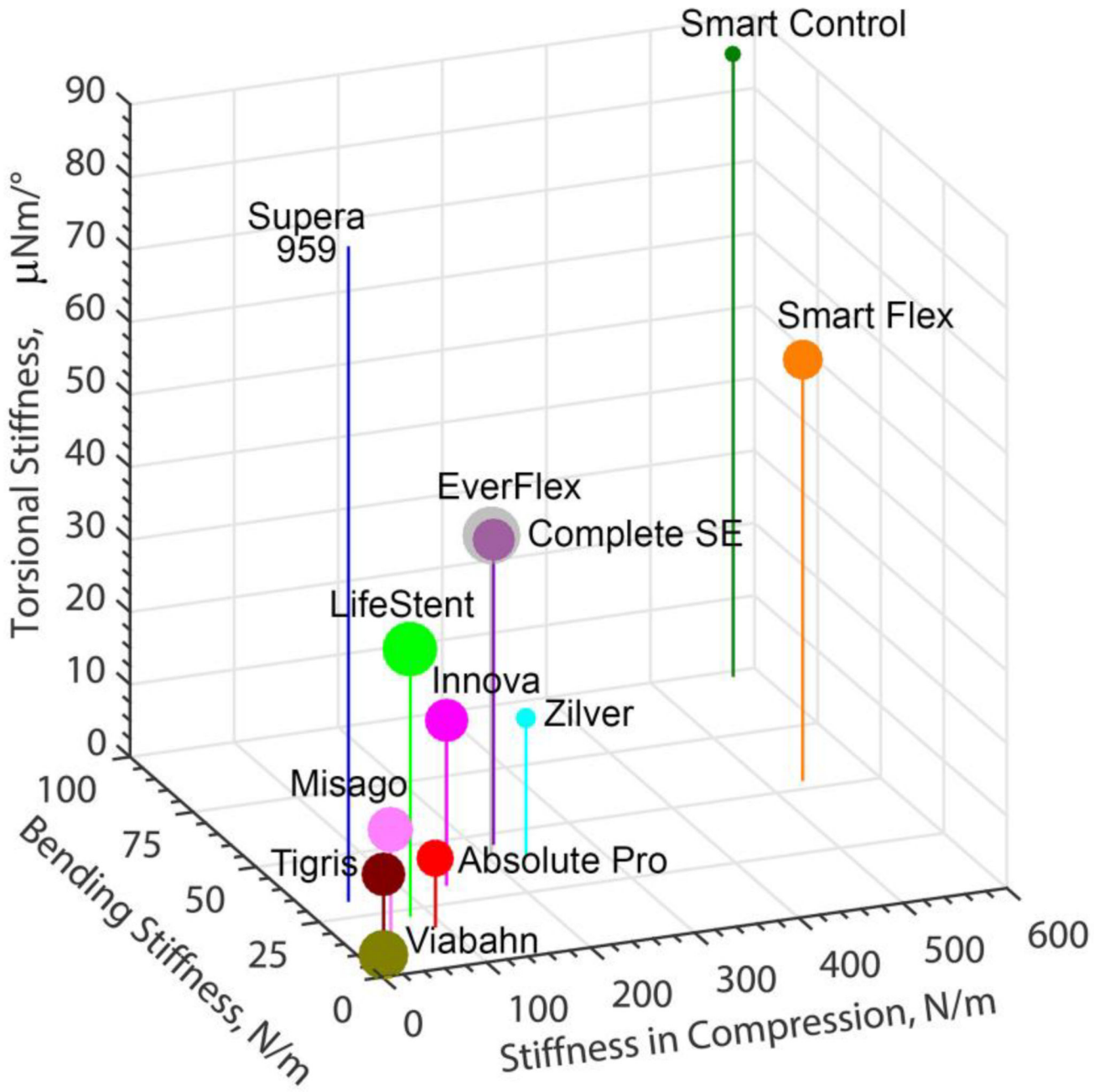


**Fig 10.**

Comparison of bending stiffness (N/m), stiffness in compression (N/m) and torsional stiffness (µN·m/°) for all stents. Size of the markers represents radial stiffness scaled down by a factor of 25 for convenience. Torsional stiffness of Supera was 959 µN·m/°.